

DETECTION OF PHAEOCYSTIS GLOBOSA IN THE BELGIAN COASTAL WATERS WITH HYPERSPECTRAL PACE/OCI SATELLITE DATA

Héloïse Lavigne¹, Kevin Ruddick¹, Quinten Vanhellemont¹, Dimitry Van der Zande¹, Dieter Vansteenkoven²

1. Royal Belgian Institute of Natural Sciences, Rue Vautierstraat 29, 1000 Brussels, Belgium
2. Flanders Marine Institute (VLIZ), Wandelaarkaai 7, 8400 Ostend, Belgium

ABSTRACT

Blooms of the phytoplankton *Phaeocystis globosa* in the Southern North Sea present significant ecological and economic challenges. Previous studies have shown that *Phaeocystis globosa* could be detected from in situ hyperspectral radiometry. In this study, we assess the potential of the new PACE/OCI hyperspectral satellite sensor to detect this species. During the 2025 spring bloom, we compared PACE/OCI data with in situ hyperspectral measurements from a PANTHYR system to evaluate *Phaeocystis globosa* detection capabilities. Using second derivative analysis, distinct spectral signatures were identified in both in situ and satellite data. The results show that PACE/OCI can successfully differentiate *Phaeocystis globosa* from diatoms blooms and that synoptic maps of the bloom can be produced. This confirms the feasibility of using hyperspectral satellite sensors for large-scale monitoring of phytoplankton species, offering a significant advancement for marine ecosystem management.

Index Terms—hyperspectral, radiometry, *Phaeocystis globosa*, PACE, Southern North Sea, satellite, phytoplankton

1. INTRODUCTION

A harmful algal bloom (HAB) is defined as the rapid development of a toxic or undesirable phytoplankton species. Monitoring of HABs can be an important task for water quality managers as timely actions may need to be taken to mitigate the associated risks. To support HAB monitoring, optical remote sensing offers valuable insights, providing information on total phytoplankton biomass with a broad regional coverage and frequent revisit times [1]. However, chlorophyll-a concentration (Chl-a hereafter) does not allow to distinguish between a non-HAB and a HAB. In this context, recently launched hyperspectral satellite sensors such as those on board PACE, EnMAP or PRISMA ([2], [3], [4]) are expected to support phytoplankton species or group-level detection [5]. Indeed, Lavigne et al. (2022) [6] demonstrated that *Phaeocystis globosa* (*P. globosa* hereafter) blooms in the southern North Sea (SNS, hereafter) can be monitored from hyperspectral radiometry using in situ data

collected by an autonomous hyperspectral radiometer system (i.e. PANTHYR [7]). However, that study also showed that retrieving the same information from satellite data is much more challenging as the phytoplankton signal is highly sensitive to interband calibration issues and signal to noise ratio.

In this study, we explore the capability of the PACE/OCI hyperspectral sensor to detect *P. globosa* bloom in the SNS. *P. globosa* is a phytoplankton species that blooms every spring in the SNS, typically proliferating after a primary bloom of diatoms due to excess of nitrate relative to silicate [8]. Although not toxic, *P. globosa* does impact the functioning of the ecosystem and human activities. *P. globosa* contributes strongly to the microbial food chain and affects fisheries and aquaculture. The deposition of foam on the beaches associated to *P. globosa* blooms presents some inconveniences for touristic and economic activities and may even be a life-threatening environment for windsurfers [9]. Consequently, the OSPAR (Oslo and Paris Commission for the Prevention of Marine Pollution) procedure which aims to assess the eutrophication status of the European waters specifically requires monitoring of this species [10].

By analyzing radiometric data from the 2025 growing season collected by an autonomous in situ PANTHYR system and by PACE satellite imagery, we aim to assess the potential of PACE data for accurate mapping of *P. globosa* blooms.

2. DATA AND METHODS

2.2. PANTHYR in situ data

A PANTHYR system [7] is deployed above water on the Blue Innovation Platform Research Tower 1 (51.24640°N, 2.91933°E), located approximately 500 m offshore of Ostend harbour in the Belgian coastal waters and operational since December 2019. The PANTHYR system is integrated in the WATERHYPERNET network (<https://waterhypernet.org/>) and consists of two TriOS/RAMESSES radiometers for radiance and irradiance mounted on a pan-and-tilt head that enables continuous radiometric measurements at specified relative azimuth to sun. A standard acquisition protocol has been designed to estimate water reflectance, see [7] and [11] for a complete description. Measurements are collected every 20

min from sunrise to sunset at $\pm 90^\circ$ and $\pm 135^\circ$ relative azimuth angles and include scans for spectral downwelling irradiance (E_d), downwelling radiance (L_d) and upwelling radiance (L_u). Data are quality checked and water reflectance (ρ_w) is calculated as described in [11]. Data from the 2025 growing season (March to June) were analyzed relying on pre-deployment sensor calibration and reanalysis modeled wind speed

2.2. Sentinel-3/OLCI satellite Chl-a data

Because of the optical complexity of the SNS which can show high turbidity and/or Chl-a concentration, the multi-algorithm Chl-a product from Lavigne et al. (2021)[12] was used. This approach switches between OC4, OC5 [13], and NIR-red [14] algorithms based on water optical conditions, making it suitable for both turbid coastal waters and offshore clear waters. This product has been extensively validated in the North Sea and is the official chlorophyll-a dataset used by OSPAR in the Quality Status Report 2023 [15].

2.3. PACE satellite data

PACE OCI Level-2 Regional Apparent Optical Properties - Near Real-time (L2_AOP_NRT, v3.0) data for the period 2025-03-20 to 2025-05-15 covering the region of interest. were downloaded from the EARTHDATA NASA website (<https://www.earthdata.nasa.gov/data>) The variable geophysical_data/Rrs was extracted from this dataset as input for *P. globosa* algorithms.

2.4. *P. globosa* detection algorithms

To investigate the presence of *P. globosa* in water reflectance data two methods were used.

The MALH index is described by [6] and is calculated from

$$MALH = \left(\frac{1}{\rho_w(\lambda_2)} - \frac{1}{\rho_w(\lambda_1)^{(1-w)}} \cdot \frac{1}{\rho_w(\lambda_3)^w} \right) \times a_w(\lambda_{NIR}) \times \rho_w(\lambda_{NIR}),$$

With $w = \frac{\lambda_2 - \lambda_3}{\lambda_1 - \lambda_3}$, (1)

In equation (1), $\lambda_1 = 470$ nm, $\lambda_2 = 482.5$ nm, $\lambda_3 = 490$ nm, $\lambda_{NIR} = 700$ nm and the water absorption at 700 nm ($a_w(\lambda_{NIR}) = 0.57$ m⁻¹, [16]). The MALH, which represents an absorption anomaly at 482.5 nm, will be positive for *P. globosa* dominated waters and negative or close to zero when *P. globosa* is at low or negligible concentration.

A second index is calculated following the Lubac et al. (2008) [17] methodology from the second derivative of reflectance, which is calculated after 5-point window running average on the water reflectance normalized by its value at 620 nm. This filter has been applied twice on PANTHYR data and 3 times for the PACE dataset.

$$\frac{d^2 \rho_{wN}}{d\lambda^2} = \frac{\rho_{wN}(\lambda_{i+1}) - 2\rho_{wN}(\lambda_i) + \rho_{wN}(\lambda_{i-1})}{(\Delta\lambda)^2}, \quad (2)$$

Where $\Delta\lambda$ is 2.5 nm for PANTHYR data and ranges between 1 and 3 nm for the PACE dataset.

Chl-a was calculated from the PANTHYR data using the NIR/red hyperspectral algorithm of [18]. This algorithm could not be applied to the PACE dataset because the reflectance spectra are truncated at 720 nm.

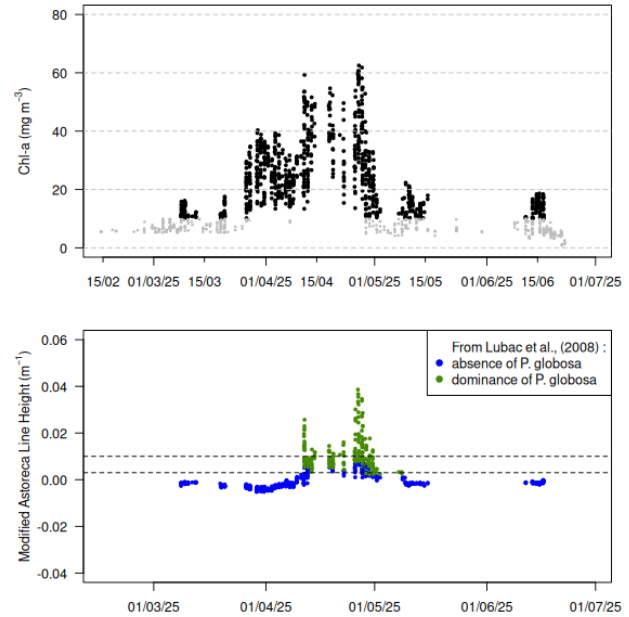


Figure 1: [top panel] Chl-a time-series calculated from the PANTHYR data. Chl-a values less than 10 mg m⁻³ are masked in grey as the retrieval algorithm [18] is not well adapted for low Chl-a values. [bottom panel] MALH calculated on the same dataset. Colour of the dots refers to the results of the Lubac et al. (2008) algorithm. The horizontal lines show the MALH domains where *P. globosa* absence (below the lower line) and presence (above the upper line) are predicted. (see [6] for details).

3. RESULTS AND DISCUSSION

Figure 1 shows the Chl-a and MALH time-series at the RT1 Ostend location for spring 2025. This result shows a main growing season from about 2025-03-25 to 2025-05-01, which can be divided into two phases.

(1) From 2025-03-25 to about 2025-04-11, Chl-a ranges from 20 to 40 mg m⁻³ and there is no detection of *P. globosa*. A diatom bloom is suspected during this period.

(2) From 2025-04-12 to 2025-05-01, Chl-a maximum increases to around 60 mg m⁻³. During this period *P. globosa* is detected with MALH exceeding 0.01 m⁻¹ and the Lubac Index suggesting dominance of *P. Globosa* when Chl-a is large.

The periods dominated by the diatoms bloom (2025-03-25 to 2025-04-01) and by the *P. globosa* bloom (2025-04-22 to

2025-04-30) are further analyzed. Figure 2 shows the second derivative of PANTHYR data at RT1 and PACE data at a position a few kilometers away (51.3°N, 2.85°E). This shifted location was chosen because RT1 is too close to the coast for the PACE/OCI resolution (see Figure 3, for the localization of RT1 and ‘shifted RT1’ on a map). Second derivative spectra show clear divergences in the 440 - 520 nm range between the diatom bloom (blue lines) and the *P. globosa* bloom (green lines). *P. globosa* spectra are characterized by a minimum around 455 nm and a maximum between 470 and 480 nm. Between 490 nm and 520 nm, the second derivative is closer to zero with local minimum observed around 505 nm for some PANTHYR and PACE spectra. The local maximum around 475 nm and the local minimum around 505 nm were

presented by [16] as the main characteristics of *P. globosa* second derivative spectra. The diatom bloom second derivative spectra are characterized by a local maximum around 465 to 470 nm and a local minimum around 485 nm. Despite the higher variability in the PACE data, similar patterns in second derivative dynamic are observed between the in situ PANTHYR data and the PACE satellite data. This observation proves that the PACE/OCI hyperspectral sensor is able to capture the small signal difference induced by pigment variations between a diatom-dominated phytoplankton bloom and a *P. globosa* phytoplankton bloom. This result opens then the door to the mapping of *P. globosa* from hyperspectral satellite sensors.

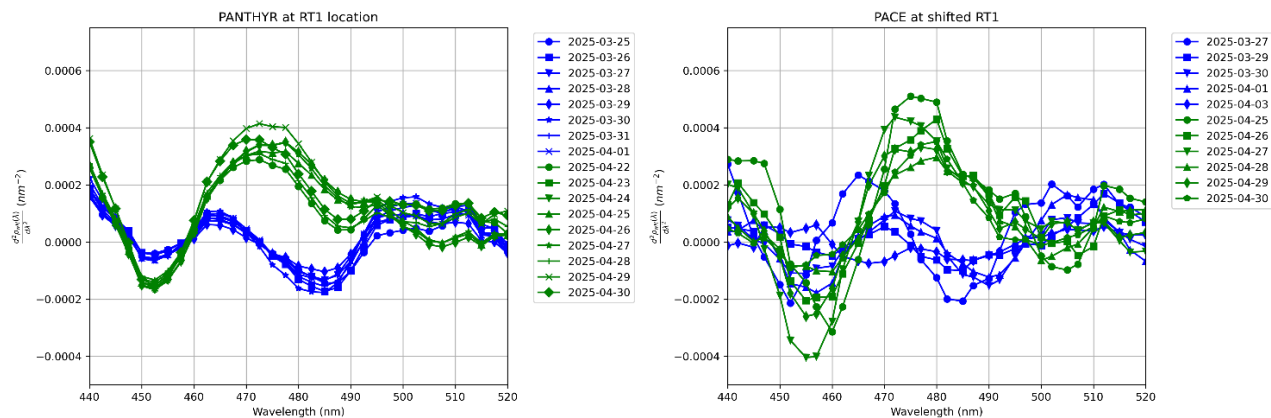


Figure 2: Second derivative of the normalized reflectance spectra during the periods identified as the diatoms bloom (blue) and the *P. globosa* bloom (green) for PANTHYR data (left) and PACE data (right). For clarity the mixed bloom period between 2025-04-03 and 2025-04-25 is not shown here.

The MALH index has been calculated for PACE images following the equation (1) and without any spatial or spectral smoothing. Satellite MALH and Chl-a imagery are presented in Figure 3 for 4 days. On 2025-03-29, Chl-a is high but MALH remains very close to 0 m⁻¹ indicating an absence of *P. globosa*. On 2025-04-11, just before *P. globosa* was identified in the PANTHYR RT1 time-series (Figure 1), imagery suggests a *P. globosa* offshore with MALH values ranging between 0.015 and 0.070 m⁻¹. This image also shows how “noisy” the MALH index is suggesting that this metric is highly sensitive to some aspect of the satellite sensor or data processing [19]. On 2025-04-26, data suggest the *P. globosa* bloom occurs close to shore as MALH shows intense values. A patch of high Chl-a is also visible near the coast. On 2025-05-12, the near shore Chl-a bloom has collapsed, although some spots with Chl-a values higher than 10 mg m⁻³ remain. These areas are also associated with higher MALH values (between 0.01 and 0.03 m⁻¹) suggesting that late and localized *P. globosa* growing events still occur after the main blooming phase. This result is also supported by the data from another PANTHYR system located at the C-POWER station

(see Figure 3 bottom left panel for its localisation) that recorded the presence of *P. globosa* from 2025-05-07 to 2025-05-15 (results not shown). The MALH maps presented in Figure 3 are consistent with *P. globosa* bloom development in Belgian coastal waters.

This study demonstrates that the PACE/OCI hyperspectral satellite sensor can successfully detect the second derivative signal of *P. globosa* in the SNS. This is a promising development for North Sea eutrophication assessment, as it enables the routine mapping of *P. globosa* blooms in the SNS. However, the *P. globosa* satellite product will need extensive analysis and validation against in situ measurements before it can be employed operationally and widely accepted by the scientific and user community.

4. CONCLUSION

This study focused on the potential of the PACE/OCI hyperspectral sensor to detect *P. globosa* blooms in the SNS, an essential component of eutrophication assessment for EU water quality [10]. Using in situ hyperspectral radiometry

data from a PANTHYR system alongside PACE satellite measurements, the results demonstrated that PACE/OCI can capture distinct spectral signatures of *P. globosa* and differentiate them from diatom blooms that generally initiate the spring bloom in the SNS. Although suggested as feasible many years ago [20], hyperspectral satellite data had not yet been conclusively demonstrated for this purpose, probably

because a high quality satellite sensor and careful data processing are needed to capture the very small optical signal. At last, the present results conclusively demonstrate that satellite data can detect *P. globosa* in this region, opening up a new perspective for large-scale, regular monitoring of *P. globosa* blooms (not just Chl-a) via satellite.

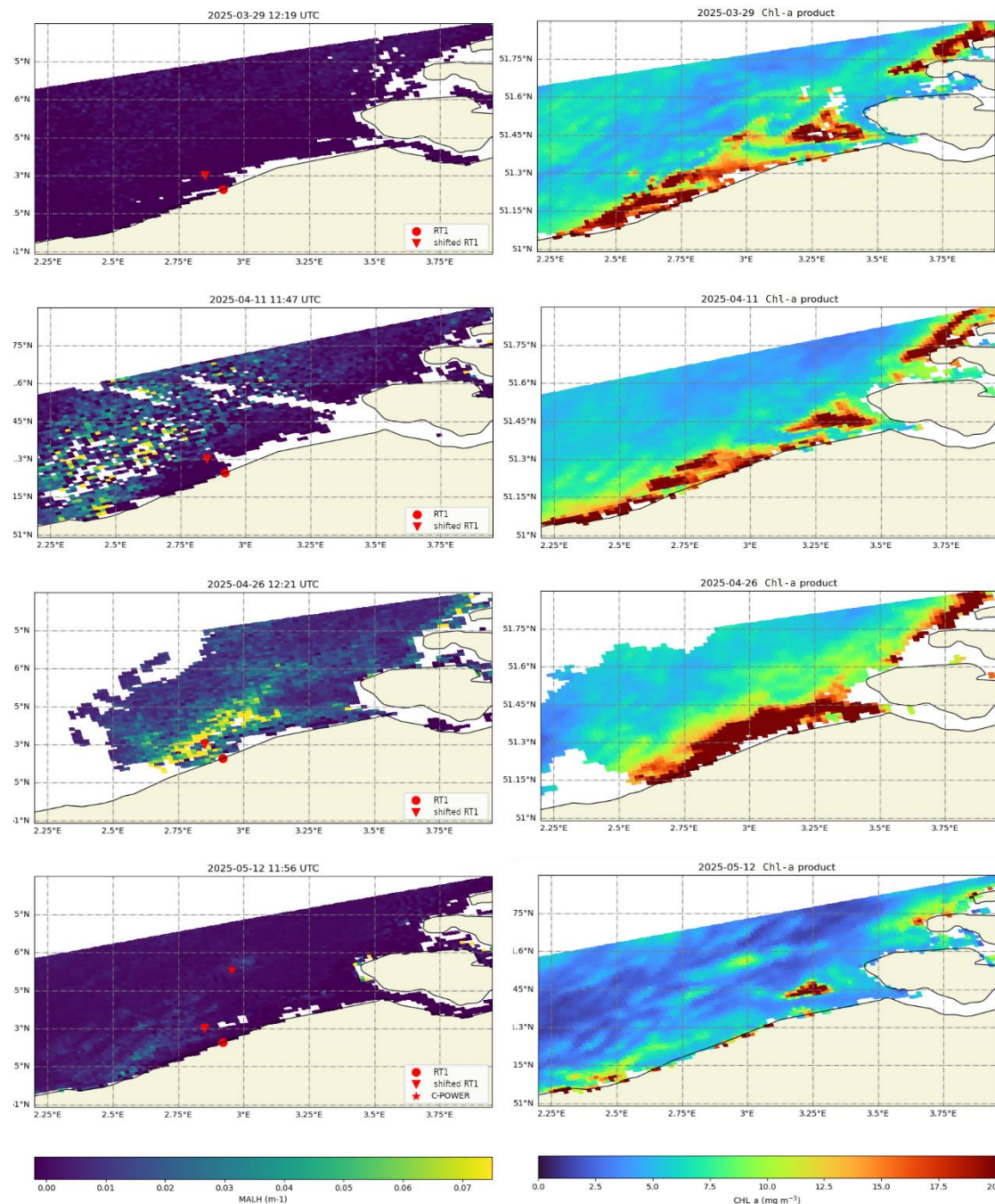


Figure 3: PACE/OCI derived MALH [left] and Chl-a concentration [right] in the Belgian coastal waters for three days during the 2025 spring bloom. The Chl-a product makes use of Sentinel3/OLCI data that are taken about 2 hours before PACE/OCI.

5. ACKNOWLEDGEMENTS

This work was funded by the European Union's Horizon 2020 research and innovation programme under grant agreement No 101081642 (project OBAMA-NEXT). The Oostende PANTHYR data was provided by the WATERHYPERNET network, funded by the European Space Agency. POM West-Vlaanderen are thanked for operating the PANTHYR on the RT1 Blue Innovation Platform (Ostend, Belgium) and installation support. Francesca Ortenzio and Matthew Beck are thanks for their work in management and maintenance of the WATERHYPERNET PANTHYR systems. NASA is acknowledged for freely providing PACE data through the EARTHDATa website.

6. REFERENCES

- [1] Stumpf, R., Culver M., Tester P., Tomlinson, M., Kirkpatrick, M., Pederson, B., Truby, E., Ransibrahmanakul, M., Soracco, M., "Monitoring *Karenia brevis* blooms in the Gulf of Mexico using satellite ocean color imagery and other data," *Harmful Algae*, vol. 2, p. 147–160, 2003.
- [2] Gorman, E., Kubalak, D., Patel, D., Mott, D., Meister, G., Werdell, P. and others, "The NASA Plankton, Aerosol, Cloud, ocean Ecosystem (PACE) mission: an emerging era of global, hyperspectral Earth system remote sensing," in *Sensors, systems, and next-generation satellites XXIII*, 2019.
- [3] Guanter, L., Segl, K., Foerster, S., Hollstein, A; Kaufmann, H., Rossner, G., Chlebek, C., Mueller, A., Storch, T., Sang, B. "Overview of the technical and scientific status of the EnMAP imaging spectroscopy mission," in *AGU Fall Meeting Abstracts*, 2015.
- [4] R. Loizzo, R., Guarini, F., Longo, T., Scopa, R., Formaro, C., Facchinetti and Varacalli, G., "PRISMA: The Italian hyperspectral mission," in *IGARSS 2018-2018 IEEE international geoscience and remote sensing symposium*, 2018.
- [5] Dierssen, H., Bracher, A., Brando, V., Loisel, H., Ruddick, K., "Data needs for hyperspectral detection of algal diversity across the globe," *Oceanography*, vol. 33, p. 74–79, 2020.
- [6] Lavigne, H., Ruddick, K., Vanhellemont, Q., "Monitoring of high biomass *Phaeocystis globosa* blooms in the Southern North Sea by in situ and future spaceborne hyperspectral radiometry," *Remote Sensing of Environment*, vol. 282, p. 113270, 2022.
- [7] Vansteenwegen, D., Ruddick, K., Cattrijsse, A., Vanhellemont, Q., Beck, M., "The pan-and-tilt hyperspectral radiometer system (PANTHYR) for autonomous satellite validation measurements—Prototype design and testing," *Remote Sensing*, vol. 11, p. 1360, 2019.
- [8] Lancelot, C., Spitz, Y., Gypens N., Ruddick, K., Becquevort, S., Rousseau, V., Billen, G. (2005). Modelling diatom and *Phaeocystis* blooms and nutrient cycles in the Southern Bight of the North Sea: the MIRO model. *Marine Ecology Progress Series*, 289, 63-78.
- [9] Philippart, K., Blauw, A., Bolhuis, H., Brandenburg, K., Brussaard, C., Gerkema, T., Herman, P., Hommersom, A., Jacobs, P., Laanen, M. and others. "Quick scan zeeschuim," http://nioz.nl/application/files/flowpaper/quick_scan_ZEESC_HUIM/#page=1 2020.
- [10] OSPAR Commission, "Trends in Blooms of Nuisance Phytoplankton Species *Phaeocystis* in Belgian, Dutch and German Waters," OSPAR Commission, London. Available at: <https://oap.ospar.org/en/ospar-assessments/intermediate-assessment-2017/pressures-human-activities/eutrophication/trends-phaeocystis-blooms/>, 2017
- [11] Vanhellemont, Q. and Ruddick, K. "Atmospheric correction of Sentinel-3/OLCI data for mapping of suspended particulate matter and chlorophyll-a concentration in Belgian turbid coastal waters," *Remote Sensing of Environment*, vol. 256, p. 112284, 2021.
- [12] Lavigne, H., Van der Zande, D., Ruddick, K., Dos Santos, J., Gohin, F., Brotas, V., Kratzer, S. "Quality-control tests for OC4, OC5 and NIR-red satellite chlorophyll-a algorithms applied to coastal waters," *Remote Sensing of Environment*, vol. 255, p. 112237, 2021.
- [13] Gohin, F., Druon, J. Lampert, L. "A five channel chlorophyll concentration algorithm applied to SeaWiFS data processed by SeaDAS in coastal waters," *International journal of remote sensing*, vol. 23, p. 1639–1661, 2002.
- [14] Gons, H., "Optical teledetection of chlorophyll a in turbid inland waters," *Environmental science & technology*, vol. 33, p. 1127–1132, 1999.
- [15] OSPAR Comission, "Eutrophication Thematic Assessment. In: OSPAR, 2023: Quality Status Report 2023." OSPAR Commission, London. Available at: <https://oap.ospar.org/en/ospar-assessments/quality-status-reports/qsr-2023/thematic-assessments/eutrophication/>, 2023
- [16] Kou, L., Labrie, D. Chylek, P. "Refractive indices of water and ice in the 0.65-to 2.5- μ m spectral range," *Applied optics*, vol. 32, p. 3531–3540, 1993.
- [17] Lubac, B., Loisel, H., Guiselin, G., Astoreca, R., Felipe Artigas, L., Mériaux, X. "Hyperspectral and multispectral ocean color inversions to detect *Phaeocystis globosa* blooms in coastal waters," *Journal of Geophysical Research: Oceans*, vol. 113, 2008.
- [18] Ruddick, K., Gons, H., Rijkeboer, R., Tilstone, G. "Optical remote sensing of chlorophyll a in case 2 waters by use of an adaptive two-band algorithm with optimal error properties," *Applied optics*, vol. 40, p. 3575–3585, 2001.
- [19] Ruddick, K., De Vis, P., Goyens, C., Kuusk, J., Lavigne, H., Vanhellemont, Q. "Second derivative water reflectance spectra for phytoplankton species detection: origin, impact, and removal of spectral wiggles," in *SPIE Conference on Remote Sensing*, Amsterdam, 2023.
- [20] Astoreca, R., Rousseau, V., Ruddick, K., Knechciak, C., Van Mol, B., Parent, J., Lancelot, C. "Development and

application of an algorithm for detecting *Phaeocystis globosa* blooms in the Case 2 Southern North Sea waters," *Journal of plankton research*, vol. 31, no. 3, pp. 287--300, 2009.